



HAL
open science

Antiwindup Input-Output Linearization Strategy for the Control of a Multistage Continuous Fermenter With Input Constraints

Céline Casenave, Marc Perez, Denis Dochain, Jérôme Harmand, Alain Rapaport, Jean-Marie Sablayrolles

► **To cite this version:**

Céline Casenave, Marc Perez, Denis Dochain, Jérôme Harmand, Alain Rapaport, et al.. Antiwindup Input-Output Linearization Strategy for the Control of a Multistage Continuous Fermenter With Input Constraints. IEEE Transactions on Control Systems Technology, 2019, 28 (3), pp.766-775. 10.1109/TCST.2019.2892932 . hal-02066978

HAL Id: hal-02066978

<https://hal.science/hal-02066978>

Submitted on 10 Jun 2022

HAL is a multi-disciplinary open access archive for the deposit and dissemination of scientific research documents, whether they are published or not. The documents may come from teaching and research institutions in France or abroad, or from public or private research centers.

L'archive ouverte pluridisciplinaire **HAL**, est destinée au dépôt et à la diffusion de documents scientifiques de niveau recherche, publiés ou non, émanant des établissements d'enseignement et de recherche français ou étrangers, des laboratoires publics ou privés.



Distributed under a Creative Commons Attribution - NonCommercial - NoDerivatives 4.0 International License

Anti-windup Input-Output linearization strategy for the control of a Multi-Stage Continuous Fermenter with Input constraints

Céline Casenave, Marc Perez, Denis Dochain, Jérôme Harmand, Alain Rapaport and Jean-Marie Sablayrolles

Abstract—The present paper deals with the control of a Multi-Stage Continuous Fermenter (MSCF) used for the study of wine fermentation. The control design is facing three main difficulties: (1) system nonlinearity; (2) lack of on-line measurement of the controlled variable (sugar concentration); (3) positive constraints on the control inputs (inlet flow rates of each tank) coming from the cascade structure of the system. A control strategy has been proposed that accounts for these specificities. It is based on an input-output linearization control law coupled with an anti-windup technique and a state observer (Kalman filter). The strategy has been tested and validated first on numerical simulations and has then been applied to the real process. The experiments gave satisfactory results that open up new perspectives on the use of the MSCF.

Index Terms—wine fermentation, cascade of reactors, control design, varying input constraints, anti-windup, input-output linearization

I. INTRODUCTION

In this paper, we consider the problem of the control of a Multi-Stage Continuous Fermenter (MSCF) used for the study of wine fermentation. The experimental setup is a set of four reactors connected in series (see Fig. 1). The objective is to control the sugar concentration in each reactor, by considering the input flow rates of the reactors as control inputs. The cascade structure of the system implies a constraint on the values of each control input. Indeed, the inlet flow rate of each reactor has to be lower than that of the preceding reactor (i.e. $Q_{i+1} \leq Q_i$). This constraint as well as the process nonlinearity make the control design complex and not trivial.

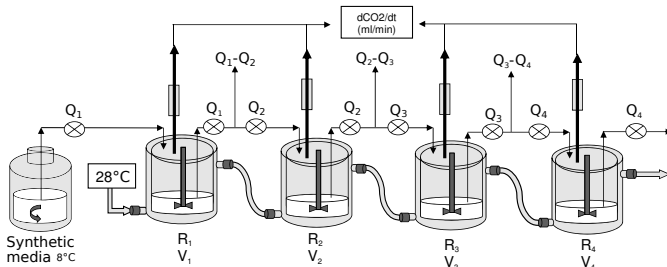


Fig. 1. Scheme of the Multi Stage Continuous Fermenter (MSCF).

The control of continuous bioreactors has been widely studied in the automatic control literature [1] with numerous applications on bioengineering processes (e.g. [2]). In comparison, only few papers deal with the issue of the control of a cascade of bioreactors (see [3], [4]) whereas such kind of devices is often used in industrial engineering processes (e.g. [5]). Moreover, only a scalar variable is

C. Casenave and A. Rapaport are with MISTEA, Univ Montpellier, INRA, Montpellier SupAgro, Montpellier, France (celine.casenave@inra.fr; alain.rapaport@inra.fr). M. Perez and J.-M. Sablayrolles are with SPO, Univ Montpellier, INRA, Montpellier SupAgro, Montpellier, France (marc.perez@inra.fr; jean-marie.sablayrolles@inra.fr). D. Dochain is with ICTEAM, Université Catholique de Louvain, Louvain-la-neuve, Belgium (denis.dochain@uclouvain.be). J. Harmand is with LBE, Univ Montpellier, INRA, Narbonne, France (jerome.harmand@inra.fr)

This work was supported in part by the 7th Framework Program of the European Union: CAFE Project (Computer-Aided Food processes for control Engineering project) - Large Collaborative Project KBBE-2007-2-3-01 and by the CEPIA division of INRA.

generally controlled in these papers. In [3] for example, the authors indeed design a controller for the glucose concentration in the process outlet. And in [4], the objective is to maximize the biogas flow rate of the first reactor in a two-stage anaerobic bioreactor, the second reactor being not controlled.

Constraints on the values of control inputs are often encountered in practice. One classical constraint is the saturation constraint with lower and upper limits on the control input u : $u_m \leq u(t) \leq u_M$. The control of system subject to saturation is the subject of numerous studies, in the case of both linear and nonlinear systems. There are generally two ways to deal with such issue: (1) either we first design a controller without taking the constraints into account and then we try to compensate the effect of the saturation (this is the case of the anti-windup techniques [6]); (2) or we include the saturation from the beginning of the design process as it is the case with set invariance control design [7] or techniques based on the polytopic representation of the saturation [8], [9]. However, these techniques are only suitable for constraints of saturation type with constant bounds. For more general forms of constraints, it is sometimes possible to make a change of variable for the control input, so that the constraint on the new input variable is a saturation. For example, the constraint $0 \leq Q_2 \leq Q_1 \leq Q_{max}$ can be replaced by $0 \leq Q_1 \leq Q_{max}$ and $0 \leq \alpha \leq 1$ where α is such that $Q_2 = \alpha Q_1$. However, when doing so, the structure of the system is modified and is often no more adapted to classical control techniques that are dedicated to particular form of systems such as control-affine systems.

Finally, it is not obvious to find control design techniques that are adapted to nonlinear systems with general positive input constraints. In [10], the author proposes to combine two techniques: the feedback linearizing control for nonlinear systems [11], and an anti-windup technique [12] for linear systems which has the advantage to handle the case of saturations with time-varying bounds. In the present paper, this control strategy has been coupled with a state observer and then applied to the MSCF. The closed loop system behaves appropriately and stabilizes faster than or at least at the same speed as when a constant input is applied. The control strategy has been validated both in numerical simulation, and on the experimental process. A first version of this strategy and the results obtained during a first set of experiments were presented at the IFAC World Congress [13]¹.

The paper is organized as follows. In Section II the experimental setup is described. The model used for the design of the control law is presented and analysed in Section III. In Section IV, the model parameters are identified and the numerical simulations are compared with experimental data for validation. Then, Section V deals with the design of the control strategy. Finally in Section VI, the control results obtained in simulation and on the experimental process are presented.

II. PROCESS DESCRIPTION

In [14] the use of a Multi-Stage Continuous Fermenter (MSCF) has been proposed to study the fermentation process. An experimental set-up has been developed by the research unit SPO (Sciences for Oenology) of INRA (Montpellier). It is composed of 4 reactors

¹The paper did receive the congress Application Paper Prize.

connected in series (see Fig. 1). The volumes V_i , $i = 1 : 4$ of the reactors are kept constant. This implies that the outlet flow rate of each reactor is equal to its inlet flow rate. The first reactor is fed with a synthetic medium which simulates a grape juice. The other reactors are fed by a fraction of the outlet medium of the preceding reactor. The inlet flow rates Q_i , $i = 1 : 4$ of the reactors are controlled independently by a pump, the only constraint (coming from the cascade structure of the device) being that the inlet flow rate Q_i of the i^{th} reactor has to be lower than the outlet flow rate Q_{i-1} of the $(i-1)^{\text{th}}$ reactor:

$$0 \leq Q_4 \leq Q_3 \leq Q_2 \leq Q_1 \leq Q_{max}, \quad (1)$$

with Q_{max} the maximal flow rate which can be applied. The temperature of the medium in each reactor is controlled at 28°C . Only the CO_2 production rate (in each of the 4 reactors) is measured on-line. A schematic view of the MSCF is given in Fig. 1.

III. MODEL DESCRIPTION AND ANALYSIS

The model of the MSCF considered in this paper is the one described in [13]. It is obtained from the model of the batch fermentation given in [15] by addition of terms related to the interconnection between the reactors. It is written:

$$\dot{\xi} = f(\xi, u) \text{ with } \xi = (\xi_1^\top, \xi_2^\top, \xi_3^\top, \xi_4^\top)^\top \quad (2)$$

and $\xi_i = (X_i, N_i, E_i, S_i)^\top$, $u = (D_1, D_2, D_3, D_4)^\top$, $f(\xi, u) = (f_1(\xi, u)^\top, f_2(\xi, u)^\top, f_3(\xi, u)^\top, f_4(\xi, u)^\top)^\top$ and $\forall i = 1 : 4$:

$$f_i(\xi, u) := \begin{bmatrix} \mu_1(N_i)X_i + D_i(X_{i-1} - X_i) \\ -k_1\mu_1(N_i)X_i + D_i(N_{i-1} - N_i) \\ \mu_2(E_i, S_i)X_i + D_i(E_{i-1} - E_i) \\ -k_2\mu_2(E_i, S_i)X_i + D_i(S_{i-1} - S_i) \end{bmatrix} \quad (3)$$

where X_i , N_i , E_i and S_i are the concentrations (in g.L^{-1}) of yeast, nitrogen, ethanol and sugar of the i^{th} reactor, respectively; $D_i = \frac{Q_i}{V_i}$ is the dilution rate of the i^{th} reactor; $(X_0, N_0, E_0, S_0) = (0, N^{in}, 0, S^{in})$ with N^{in} , $S^{in} > 0$ are the concentrations of yeast, nitrogen, ethanol and sugar in the inlet medium; and k_1 and k_2 are the yield coefficients. The functions μ_1 and μ_2 are given by:

$$\mu_1(N) = \frac{\mu_1^{max} N}{K_N + N}, \quad \mu_2(E, S) = \frac{\mu_2^{max} S}{K_S + S} \frac{K_E}{K_E + E}, \quad (4)$$

with μ_1^{max} , μ_2^{max} , K_S , K_N and K_E the maximum specific growth rates of the two reactions, the half-saturation constants of the Monod laws, and the inhibition constant respectively. To complete the model, the following initial conditions are considered: $\forall i = 1 : 4$,

$$X_i(0) = X^{in}, N_i(0) = N^{in}, E_i(0) = 0, S_i(0) = S^{in}. \quad (5)$$

We also denote C_i the CO_2 production rate of the i^{th} reactor:

$$C_i(\xi) := \mu_2(E_i, S_i)X_i. \quad (6)$$

Let us now give a few analysis results about the MSCF model (2). The goal is only to show that the model is consistent with some biological laws and experimental observations. The proofs of the results, long but only technical, are not given in this paper.

By simple computations, we can first show that the set Ω defined by:

$$\Omega := \left\{ \xi \in \mathbb{R}^{16} \text{ such that } \begin{cases} 0 \leq X_i \leq \frac{N^{in} - N_i}{k_1} \\ 0 \leq N_i \leq N^{in} \\ 0 \leq E_i \leq \frac{S^{in} - S_i}{k_2} \\ 0 \leq S_i \leq S^{in} \end{cases} \right\} \subset \mathbb{R}_+^{16} \quad (7)$$

(with $\mathbb{R}_+^{16} = [0, +\infty[^{16}$), is a positive invariant set of system (2), which proves its consistency with the mass balance conservation law.

One can also easily show that, if $\frac{Q_1}{V_1} < \mu_1(N^{in})$, then the system (2) admits a unique positive and locally exponentially stable steady state $\xi^* \in \Omega$; moreover this steady state is such that:

$$0 < S_i^* < S_{i-1}^* \text{ and } X_i^* > X_{i-1}^*, \forall i = 1 : 4 \quad (8)$$

with $S_0^* = S^{in}$ and $X_0^* = X^{in}$. It means that, providing that $Q_{max} < V_1\mu_1(N^{in})$, all inlet flow rate values (Q_1, Q_2, Q_3, Q_4) that meet the constraint (1) will make the system stabilize at a positive equilibrium point without any washout in all the reactors ($X_i^* \neq 0, \forall i$).

However, given $(\bar{S}_1, \bar{S}_2, \bar{S}_3, \bar{S}_4) \in [0, S^{in}]^4$ with $\bar{S}_1 > \bar{S}_2 > \bar{S}_3 > \bar{S}_4$, it does not necessarily exist some values $(Q_1, Q_2, Q_3, Q_4) \in [0, V_1\mu_1(N^{in})]^4$ with $Q_4 \leq Q_3 \leq Q_2 \leq Q_1$ such that the equilibrium point ξ^* of system (2) verifies $S_i^* = \bar{S}_i, \forall i = 1 : 4$. An example of set of reachable values of sugar concentrations is given in Fig. 2.

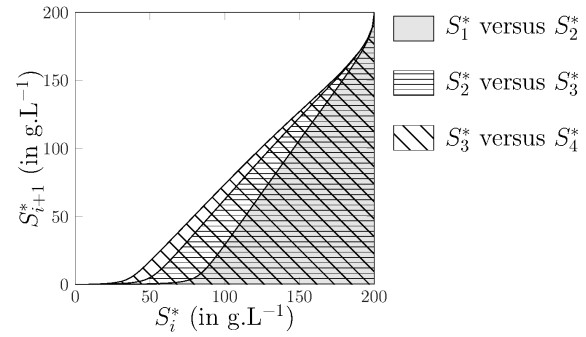


Fig. 2. Example of set of reachable values of sugar concentrations at equilibrium in the MSCF.

IV. MODEL IDENTIFICATION

Let us first focus on the estimation of the value of the initial sugar concentration S^{in} that plays a key role. In the model of the batch fermentation (model (2) with $D_i = 0$), it is assumed that the yield coefficient k_2 is constant during the fermentation. However, it is well-known in the field of Oenology that k_2 varies: in particular, it is smaller at the beginning of the fermentation (see table I). Fortunately

TABLE I

ESTIMATED VALUES OF THE YIELD COEFFICIENT $k_2 = \frac{E}{S^{in} - S}$ from measured values of E and S during a batch fermentation. $k_2^{(1)}$ is obtained with $S^{in} = 200 \text{ g.L}^{-1}$ and $k_2^{(2)}$ with $S^{in} = 195.8 \text{ g.L}^{-1}$.

t [h]	16.4	20.9	24.0	26.1	40.5	45.7	49.4	65.4	74.9
$k_2^{(1)}$	0.339	0.432	0.434	0.437	0.464	0.457	0.461	0.463	0.463
$k_2^{(2)}$	0.449	0.494	0.472	0.468	0.480	0.470	0.473	0.474	0.473

this variation of k_2 can be artificially attenuated by a modification of the value of S^{in} in the model. Indeed at the beginning of the fermentation the quantity $S^{in} - S$, which represents the concentration of sugar that has been consumed, is small. A slight decrease of the value of S^{in} will then lead to an increase of the value of $k_2 = \frac{E}{S^{in} - S}$ larger than the increase obtained at the end of the fermentation where the value of $S^{in} - S$ is large (close to S^{in}). By decreasing slightly the value of S^{in} in the model, we can therefore keep a constant value of k_2 without degrading too much the accuracy of the model.

In the case of the batch fermentation data set considered in table I, the value of S^{in} that enables to attenuate at best the variation of k_2 is equal to 195.8 g.L^{-1} , which is 4.2 g.L^{-1} smaller than the real value of 200 g.L^{-1} . This value, denoted \bar{S}^{in} in the sequel, has been

obtained by simple linear regression between S and E ($R^2 = 0.999$) based on the relationship $S = S^{in} - k_2 E$.

For the parameter identification we used a data set collected by the unit SPO [14]. Each experiment consisted in the application of a set of constant inlet flow rates Q_i , $i = 1 : 4$ that fulfill the constraint (1); after stabilization, the equilibrium values of the concentrations of yeast, sugar, ethanol and nitrogen were measured.

The value of parameter k_2 was considered as known as it is a stoichiometric coefficient of a well-known chemical reaction; we used the value given in [15]. The other parameters of model (2) were identified from the experimental data: a simplex method was used to minimize the sum of the squares of the distances between the experimental measurements at equilibrium in the 4 stages of the MSCF and the values obtained by numerical simulation of the model. Because the equations of the nitrogen and yeast concentrations are independent of the other ones, the identification was performed in two steps: (1) first the coefficients k_n , k_1 and μ_1^{max} were identified from the measurements of the yeast concentrations; (2) then the coefficients k_s , k_e and μ_2^{max} were identified from the measurements of the sugar concentrations. The values of the identified parameters are given hereafter²:

$$\begin{aligned} k_1 &= 0.068, k_2 = 2.17, \mu_1^{max} = 0.75 [\text{h}^{-1}], \mu_2^{max} = 1.746 [\text{h}^{-1}] \\ k_n &= 0.714 [\text{g.L}^{-1}], k_s = 0.884 [\text{g.L}^{-1}], k_e = 13.8 [\text{g.L}^{-1}] \end{aligned} \quad (9)$$

The comparison between the experimental data used for the identification process, and the values obtained by simulation with the parameter values (9) is given in Fig. 3 (top). For the cross validation, we compared simulated trajectories of a batch fermentation with experimental data (Fig. 3 (bottom)). In both cases, the simulation give results close to the measured values.

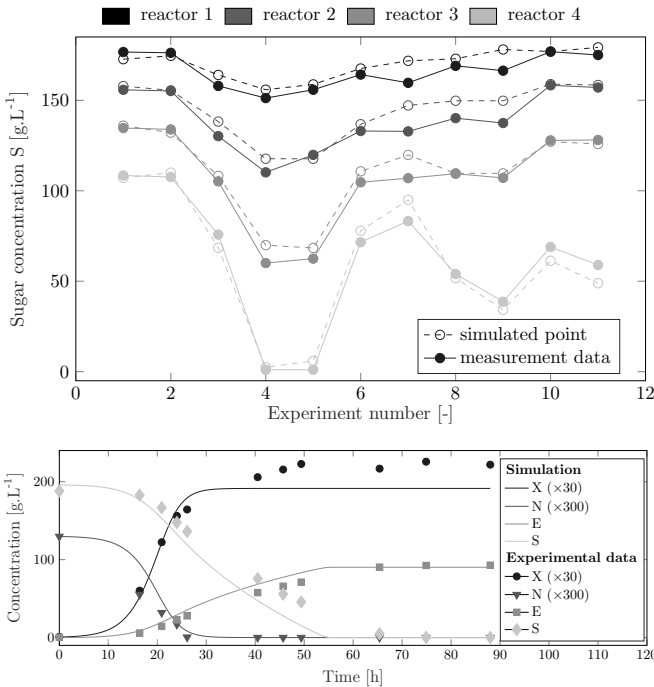


Fig. 3. Comparison between experimental data and simulations of the models of fermentation (batch and MSCF). Top: sugar concentration values at equilibrium in the MSCF. The experimental data are the ones used for the identification process. Bottom: yeast, nitrogen, ethanol and sugar concentrations of a batch fermentation (cross validation).

² k_1 and k_2 are dimensionless parameters.

V. DESIGN OF THE CONTROL LAW

Recall that the objective is to control the sugar concentration in each stage of the MSCF, the control inputs being the inlet flow rates Q_i , $i = 1 : 4$, of the 4 reactors. In the sequel, we denote S_i^* the value of the sugar concentration setpoint in the i^{th} reactor (for $i = 1 : 4$). We only consider setpoint values such that there exist constant input control values $(Q_1^*, Q_2^*, Q_3^*, Q_4^*) \in [0, Q_{max}]^4$ verifying the constraint (1) and which, when applied to system (2), stabilize the sugar concentrations in the 4 reactors at the values S_i^* , $i = 1 : 4$. This implies that $S^{in} > S_1^* > S_2^* > S_3^* > S_4^* > 0$ and $Q_{max} < V_1 \mu_1(N^{in})$ (see section III). Thus, after stabilization, it is possible to switch to constant input flow rates in order to maintain the system in the same state without applying the closed loop control law.

The control design is facing two main difficulties: on one hand, no on-line measurement of the sugar concentration is available, and on the other hand the control inputs Q_i have to verify the constraint (1). The proposed control strategy is based on a linearizing control law, coupled with an anti-windup component and a state observer. A scheme of the control strategy is given in Fig. 4b.

A. Linearizing control law

To account for the system nonlinearities, a linearizing control law is considered. The equation of S_i has a relative degree equal to 1 with respect to Q_i ; the control law is therefore written³:

$$Q_i = V_i \frac{k_2 C_i + v_i}{S_{i-1} - S_i} := \Psi_i(v_i, S, C), \quad (10)$$

where $C = (C_1, C_2, C_3, C_4)^T$, $S = (S_1, S_2, S_3, S_4)^T$ and v_i is the expression of the desired closed loop dynamics of S_i . Here we consider a simple proportional-integral linear dynamics:

$$v_i = a_{i,1}(S_i^* - S_i) + a_{i,2} \int_0^t (S_i^* - S_i(\tau)) d\tau, \quad (11)$$

with $a_{i,1}$ and $a_{i,2}$ some positive constants. The integral term is introduced to compensate modeling and measurement errors. Note that the control law (10) is independent of the function μ_2 because the quantity C_i is measured on-line.

B. Saturation

Consider the saturation operator defined by:

$$\text{sat}(u; u_m, u_M) := \begin{cases} u_M & \text{if } u \geq u_M \\ u & \text{if } u_m < u < u_M \\ u_m & \text{if } u \leq u_m. \end{cases} \quad (12)$$

Compared to problems often considered in the literature, the constraints on the control inputs of our system are coupled and time-varying. We chose to apply the saturation operator (12) to one control input after the other. The choice of the saturation order of the 4 control inputs Q_i is not obvious: it can lead to very different control performances, depending on the setpoints, the initial conditions, and the experimental conditions. The 14 possible saturation orders are given in Table II, $n_i = j$ meaning that Q_i will be the j^{th} control input to be saturated.

For example, the order $n^{\circ 8}$ has to be understood as follows:

1. $n_3 = 1 \implies \tilde{Q}_3 = \text{sat}(Q_3; 0, Q_{max})$
2. $n_1 = n_4 = 2 \implies \begin{cases} \tilde{Q}_1 = \text{sat}(Q_1; \tilde{Q}_3, Q_{max}) \\ \tilde{Q}_4 = \text{sat}(Q_4; 0, \tilde{Q}_3) \end{cases}$
3. $n_2 = 3 \implies \tilde{Q}_2 = \text{sat}(Q_2; \tilde{Q}_3, \tilde{Q}_1)$

This saturation strategy can be written as follows:

³Note that this control law can not be applied if $S_i = S_{i-1}$, case that never happens except at the very beginning of the experiments when the reactors are filled with the must and then connected to each other.

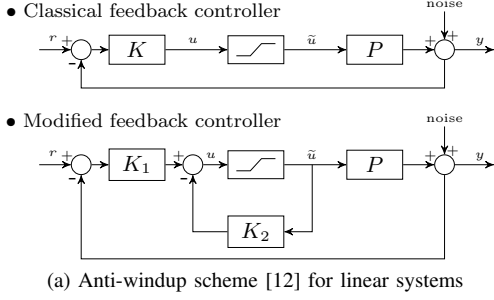


Fig. 4. Schemes of control strategies.

TABLE II
THE 14 POSSIBLE SATURATION ORDERS.

	1	2	3	4	5	6	7	8	9	10	11	12	13	14
n_1	1	1	1	1	1	2	2	2	3	2	2	3	4	3
n_2	2	2	3	3	4	1	1	3	2	3	4	2	3	4
n_3	3	4	2	4	3	2	3	1	1	4	3	3	2	2
n_4	4	3	3	2	2	3	2	2	2	1	1	1	1	1

$$\tilde{Q}_i = \text{sat}(Q_i; Q_{i,m}, Q_{i,M}), \quad (13)$$

where $Q_{i,m} = \max_{j>i, n_j < n_i} \tilde{Q}_j$ and $Q_{i,M} = \min_{j<i, n_j < n_i} \tilde{Q}_j$, with $\tilde{Q}_5 = 0$, $\tilde{Q}_0 = Q_{max}$ and $n_0 = n_5 = 0$.

C. Anti-windup

Enforcing input control constraints by application of a saturation operator can result in poor closed-loop performances and overshooting of the integral term. To minimize the performance loss, some anti-windup control schemes have been developed. However, the problems studied in the literature are most of the time linear. An interesting solution for nonlinear systems was proposed in [10]. It is based on the combination of two techniques: the feedback linearizing control for nonlinear systems [11], and the anti-windup technique developed by Zheng et al [12], which has the advantage to handle the case of saturations with time-variable bounds. The combined scheme is explained here after.

• Anti-windup technique of Zheng et al [12] for linear systems

Consider a linear and stable square system of transfer function P that is subject to input saturation constraint⁴:

$$y = P\tilde{u} \text{ with } \tilde{u} = \text{sat}(u; u_m, u_M) \quad (14)$$

where y , u and \tilde{u} are the output, input and saturated input of the system respectively. Let K be a feedback controller designed on the unconstrained system (see Fig. 4a), r the setpoint and F a diagonal filter such that FP is bi-proper (that is a rational function with the same numerator and denominator degrees). The input \tilde{u} that fullfills the saturation constraint and which is such that at each time t :

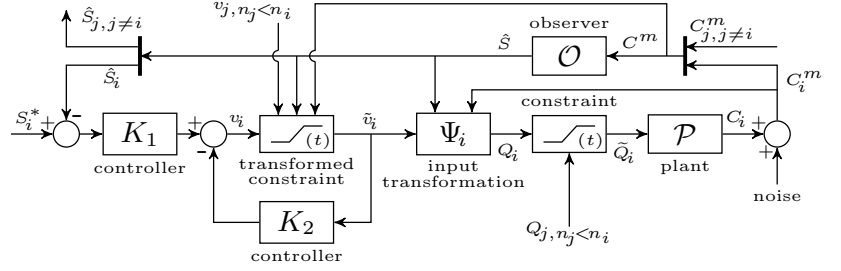
$$\tilde{u}(t) = \underset{\tilde{v}(t)}{\text{argmin}} \left| [FP(I + KP)^{-1}Kr](t) - [FP\tilde{v}](t) \right|_1 \quad (15)$$

is given by (see Fig. 4a):

$$\tilde{u} = \text{sat}(K_1(r - y) - K_2\tilde{u}; u_m, u_M) \quad (16)$$

with $K_1 = FP(I + KP)^{-1}K$ and $K_2 = FP - I - K_1P$. At each time instant, this saturated control input minimizes the difference

⁴In the sequel, by abuse of notation and for simplicity, the Laplace transform of a function f will be denoted itself by f when there is no ambiguity.



between the output of the closed loop system without saturation and the output of the system obtained with the saturated input.

To guarantee the internal stability of the closed loop system and the implementability of controller, the following assumptions have to be verified:

- 1) $(I + KP)^{-1}K$ is bi-proper, minimum phase and stable,
- 2) $FP|_{s=\infty}$ is a diagonal nonsingular matrix with finite elements,
- 3) K_1 is minimum phase and stable,
- 4) $K_1P + K_2$ is strictly proper.

• Adaptation to nonlinear systems by Doyle [10]

Let now consider affine nonlinear SISO systems of the form:

$$\frac{dx}{dt} = f(x) + g(x)u; \quad y = h(x), \quad (17)$$

subject to input saturation: $u_m \leq u \leq u_M$.

The first step of the control strategy is an Input-Output linearization that consists in a change of input variable of the form:

$$u = f_1(x) + f_2(x)v, \quad (18)$$

where f_1 and f_2 are chosen in such a way that the system with input v and output y is linear: $y = Pv$ with P a rational transfer function.

Then the initial constraint on u is transformed in a constraint on v in the following way:

$$\begin{aligned} u_m \leq u := f_1(x) + f_2(x)v \leq u_M \\ \Leftrightarrow \frac{u_m - f_1(x)}{f_2(x)} \leq v \leq \frac{u_M - f_1(x)}{f_2(x)}. \end{aligned} \quad (19)$$

Finally the antiwindup scheme proposed by Zheng et al in [12] is applied to the linear system $y = Pv$ with the time-varying input constraint (19).

• Application to the MSCF

The input-output linearization, already presented in section V-A, is obtained with the change of variables (10) that is of the form (18) with $f_1(x) = V_i \frac{k_2 C_i}{S_{i-1} - S_i}$ and $f_2(x) = \frac{V_i}{S_{i-1} - S_i}$. The resulting transfer function between v_i and S_i is $P(s) = \frac{1}{s}$.

The constraint on Q_i is then transformed into a constraint on v_i :

$$\begin{aligned} Q_{i,m} < Q_i < Q_{i,M} \\ \Leftrightarrow \underbrace{\frac{S_{i-1} - S_i}{V_i} Q_{i,m} - k_2 C_i}_{v_{i,m}} < v_i < \underbrace{\frac{S_{i-1} - S_i}{V_i} Q_{i,M} - k_2 C_i}_{v_{i,M}}. \end{aligned} \quad (20)$$

To apply the anti-windup scheme of Zheng et al [12] to the linear system of transfer function $P(s) = \frac{1}{s}$ with the input saturation constraint (20), we first have to consider a feedback controller for the unconstrained problem. The controller we have chosen is the one expressed in (11) which is written in the frequency domain:

$$v_i = K(S_i^* - S_i) \text{ with } K(s) = \frac{a_{i,1}s + a_{i,2}}{s}. \quad (21)$$

Several controllers for the constrained problem can then be proposed, following the method of Zheng et al [12]. The choice of $F(s) = a_{i,1} \frac{s^2 + a_{i,1}s + a_{i,2}}{a_{i,1}s + a_{i,2}}$ leads to the following controllers:

$$K_1 = FP(I + KP)^{-1}K = a_{i,1} \quad (22)$$

$$K_2 = FP - I - K_1P = -\frac{a_{i,2}}{a_{i,1}s + a_{i,2}}, \quad (23)$$

which check all the assumptions required provided that $a_{i,1}, a_{i,2} > 0$.

By applying the same saturation order as for the Q_i values ($i = 1 : 4$), we then finally have:

$$\tilde{v}_i = \text{sat}(v_i; v_{i,m}, v_{i,M}) \text{ with } v_i = K_1(S_i^* - S_i) - K_2\tilde{v}_i. \quad (24)$$

D. Observer

The anti-windup control scheme presented in the previous paragraphs assumes a full knowledge of both the sugar concentrations S_i and the CO_2 production rate C_i in each reactor. However, only the CO_2 production rate is measured on-line. To get an on-line estimate of the sugar concentration, we need to use a state observer. Several observation strategies (among which the asymptotic observer [13] and the extended Kalman Filter) have been tested numerically, which all give similar results. They also all have the same drawback: the convergence rate is always limited by the value of D_i .

Finally, we chose to use a Continuous-Discrete Extended Kalman Filter (see [16] pp.664), as it seemed to handle better uncertainties on the observer initial condition. This approach is dedicated to continuous time model of the form (2), with an additional discrete-time measurement output equation of the form:

$$C_k^m = C(\xi(t_k)) + \eta_k, \quad (25)$$

where, in our case, $C(\xi) = (C_1(\xi), C_2(\xi), C_3(\xi), C_4(\xi))^T$, and η_k is a Gaussian measurement noise of zero mean and covariance matrix R_k assumed to be equal to $R_k = \sigma I_4$ with $\sigma > 0$ (I_4 being the identity matrix of size 4×4). No noise was added in the model equations. At each time instant t_k , the Kalman Filter computes an estimation of the state $\hat{\xi}_k^+$ and of the error covariance matrix P_k^+ in two steps: a first step of prediction based on the model and the previous estimated values, and a second step of correction based on the measurement.

For the initial value of the state estimate $\hat{\xi}_0^+$, we took advantage of the fact that, at the observer initialization time $t_k = 0$, the system is assumed to be at equilibrium. Indeed, in practice, the control law will be used to go from one equilibrium point to another. Under this assumption, we get from (2) the following estimation $\hat{\xi}_0^+$ of $\xi(0)$:

$$\hat{\xi}_0^+ = (\hat{\xi}_{1,0}^+, \hat{\xi}_{2,0}^+, \hat{\xi}_{3,0}^+, \hat{\xi}_{4,0}^+)^T \text{ with } \hat{\xi}_{i,0}^+ = (\hat{X}_i^0, \hat{N}_i^0, \hat{E}_i^0, \hat{S}_i^0)^T, \quad (26)$$

and $\forall i = 1 : 4$,

$$\hat{S}_i^0 = -k_2 \frac{C_i^m(0)}{D_i(0)} + \hat{S}_{i-1}^0, \quad \hat{E}_i^0 = \frac{C_i^m(0)}{D_i(0)} + \hat{E}_{i-1}^0, \quad (27)$$

$$\hat{X}_i^0 = \frac{C_i^m(0)}{\mu_2(\hat{E}_i^0, \hat{S}_i^0)}, \quad \hat{N}_i^0 = \frac{K_N D_i(0)(\hat{X}_i^0 - \hat{X}_{i-1}^0)}{\mu_1^{max} \hat{X}_i^0 - D_i(0)(\hat{X}_i^0 - \hat{X}_{i-1}^0)}, \quad (28)$$

where $C_i^m(0)$ is the measurement of $C_i(0)$ and $\hat{S}_0^0 = S^{in}$, $\hat{E}_0^0 = 0$ and $\hat{X}_0^0 = 0$. The initial value P_0^+ has then been classically chosen equal to $\varepsilon \times P_0^2$ with $\varepsilon > 0$ and P_0 the 16×16 diagonal matrix whose diagonal vector is ξ_0^+ .

In practice, some off-line measurements of the sugar concentration are available during the experiment. The information given by these measurements, even if they are available only a few hours after the sampling, can be used to adjust the estimation of the observer. It can be very useful, especially to correct the error made on the initial conditions of the observer. In the experiments presented in section VI, three off-line measurements of the sugar concentrations are performed

at different times. For an other example, the reader can refer to the conference paper [13] where the adjustment of the observer (which is not a Kalman Filter) is more visible.

E. Complete control strategy scheme

Finally, the complete control strategy is written (Fig. 4b) :

$$\hat{S}_i \quad \text{given by the Extended Kalman Filter} \quad (29)$$

$$v_i = K_1(S_i^* - \hat{S}_i) - K_2\tilde{v}_i, \quad (30)$$

$$\tilde{v}_i = \text{sat}(v_i; v_{i,m}, v_{i,M}), \quad (31)$$

$$Q_i = \Psi_i(\tilde{v}_i, \hat{S}_i, C^m), \quad (32)$$

$$\tilde{Q}_i = \text{sat}(Q_i; Q_{i,m}, Q_{i,M}). \quad (33)$$

It takes less than 4 milliseconds to compute the value of the control input from the new online measurements of the CO_2 production rate.

VI. NUMERICAL AND EXPERIMENTAL VALIDATIONS

The control strategy was validated in numerical simulations and applied to the experimental setup. The results are given hereafter.

A. Design of the experiments

The considered MSCF has 4 reactors of respective volumes:

$$(V_1, V_2, V_3, V_4) = (1, 0.8, 0.55, 0.7) \text{ [L]}. \quad (34)$$

The maximal value of inlet flow rate that can be applied is $Q_{max} = 0.24 \text{ L.h}^{-1}$. The synthetic media contains $S_{in} = 202 \text{ g.L}^{-1}$ of glucose (quantity measured at the beginning of the experiments) and $N_{in} = 0.425 \text{ g.L}^{-1}$ of assimilable nitrogen. At the beginning of the experiment, the yeasts are inoculated in each reactor, with an initial concentration X_{in} of 10^6 cell/mL which corresponds to 0.04 g.L^{-1} for the yeast strain used (commercial strain EC1118, Lallemand SA).

The setpoint we consider for the experiments is the following one:

$$(S_1^*, S_2^*, S_3^*, S_4^*) = (170, 140, 110, 70) \text{ [g.L}^{-1}\text{]}; \quad (35)$$

its reachability has been verified in simulation (see next paragraph).

To avoid the case where $Q_{i+1} = Q_i$ for which we have observed a significant difference between the inlet flow rate values to be applied, and the real measured inlet flow rates, the constraint (1) was replaced by the stronger following one:

$$Q_1 < Q_{max} \text{ and } \forall i = 2 : 4, 0 < Q_i < 0.9 Q_{i-1}. \quad (36)$$

The saturation strategy (section V-B) was modified consequently.

We assume that, when the control law is applied, the MSCF is at equilibrium, the constant dilution rates being equal to:

$$(D_1^0, D_2^0, D_3^0, D_4^0) = (0.24, 0.26, 0.32, 0.05) \text{ [h}^{-1}\text{]}. \quad (37)$$

It corresponds to the following values of inlet flow rates:

$$(Q_1^0, Q_2^0, Q_3^0, Q_4^0) = (0.24, 0.208, 0.176, 0.035) \text{ [L.h}^{-1}\text{]} \quad (38)$$

that fulfill the constraint (36).

B. On-line measurements of the CO_2 production rate

The control strategy relies on the availability of an on-line measurement of the CO_2 production rate C in each stage of the MSCF. In our experiments, we measured the CO_2 present in the gas released in the air by the fermentation process and we deduced from this measurement an estimation of the CO_2 gaseous outflow rate (quantity of CO_2 released by unit of time); a new measurement is available every 20 minutes. We then assumed that at each time t , the CO_2 gaseous outflow rate is equal to the CO_2 production rate. However, it is well-known that a part of the CO_2 produced by the degradation of

sugar during the fermentation process is dissolved in the grape juice: this quantity can therefore not be measured from the produced gas that only contains the released CO_2 . This bias on the measurement of the CO_2 induces an error on the estimation of the CO_2 production rate at the beginning of the fermentation, when the medium is not saturated in CO_2 . After this period, the CO_2 gaseous outflow rate gives a good estimation of the CO_2 production rate. We will see in the sequel how to compensate this error in the model.

The model of the batch fermentation (model (2) with $D_i = 0$), and the associated control strategy, rely on a strong relationship between the sugar concentration S and the CO_2 ; we indeed have:

$$\forall t > 0, \frac{dS}{dt} = -k_2 \frac{dCO_2}{dt} \Leftrightarrow S(t) = \bar{S}^{in} - k_2 CO_2(t). \quad (39)$$

Thus, a measurement error made on $CO_2(t)$ directly impacts the estimation of $S(t)$. Let denote by c_d the quantity of CO_2 dissolved in the medium (in $g.L^{-1}$) and $CO_2^m(t)$ the measured value of CO_2 at time t ; then we have: $CO_2(t) = CO_2^m(t) + c_d$ which leads to:

$$S(t) = \tilde{S}^{in} - k_2 CO_2^m(t) \text{ with } \tilde{S}^{in} = \bar{S}^{in} - k_2 c_d. \quad (40)$$

By removing from \bar{S}^{in} the quantity of sugar corresponding to the quantity of dissolved CO_2 , we can therefore compensate the measurement error on CO_2 providing that we know the value of c_d .

To obtain an order of magnitude of c_d , we can perform a linear regression between E and CO_2^m , based on the relationship $E = CO_2 = CO_2^m(t) + c_d$. Indeed the measurement of the ethanol concentration is not biased on the contrary of the measurement of CO_2 . The least squares regression performed on the batch fermentation data set of Fig. 3 leads to the value of $c_d = 3.99 g.L^{-1}$ with $R^2 = 0.9985$, which corresponds to a sugar concentration value $k_2 c_d = 8.7 g.L^{-1}$. To compensate the measurement bias on CO_2 in the model, we can therefore decrease the value of \bar{S}^{in} of $8.7 g.L^{-1}$. Recall that \bar{S}^{in} was obtained from S^{in} by subtraction of $4.2 g.L^{-1}$ to attenuate the variability of k_2 (see section IV). So the quantity \tilde{S}^{in} can be seen as a corrected value of S^{in} that takes into account two corrections: a first one to attenuate the variability of k_2 and a second one to compensate the measurement bias on CO_2 .

As the MSCF behaves slightly differently from the batch fermentation process, a new value of \tilde{S}^{in} has been computed from the data set obtained with the MSCF. In Fig. 5, the measured CO_2 gaseous outflow rate is plotted versus the fermentation progress $1 - S/S^{in}$ where $S^{in} = 202 g.L^{-1}$. The value of S was either measured or estimated. The measurements of S were mainly made at equilibrium in the different reactors of the MSCF, except for one measurement performed at the end of the growth phase during a batch fermentation. The estimated values of S during a batch fermentation were deduced from CO_2^m by the formula $S = \tilde{S}^{in} - k_2 CO_2^m$ for two values of \tilde{S}^{in} : $202 g.L^{-1}$ and $182 g.L^{-1}$. As we can see, the estimated values of S obtained with $\tilde{S}^{in} = 182 g.L^{-1}$ give much better results than the other ones. The value of \tilde{S}^{in} can obviously be adjusted more precisely either by an off-line estimation or even by an on-line estimation (with a Kalman Filter for example). In the experiments presented in section VI-D the value of $182 g.L^{-1}$ was used, which improved greatly the results compared to the one presented in [13].

In the sequel we will no more distinguish the CO_2 gaseous outflow rate from the CO_2 production rate for simplicity.

C. Numerical tests

For the numerical experiments, we used different parameter sets for the control law and for the simulation of the MSCF to which we apply the control law, in order to test the robustness to parameter uncertainty of the control strategy. The parameter set used for the

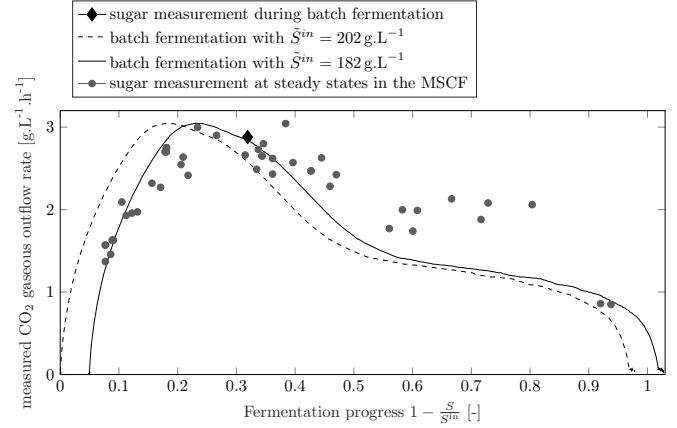


Fig. 5. Plot of the measured CO_2 gaseous outflow rate versus the fermentation progress $1 - \frac{S}{S^{in}}$ with $S = \tilde{S}^{in} - k_2 CO_2$ for $S^{in} = 202 g.L^{-1}$ and for different values of \tilde{S}^{in} during some batch fermentations. Comparison with some sugar measurement data.

control law is the one given in (9). The one used for the simulation of the MSCF is given by:

$$\begin{aligned} k_1 &= 0.0606, k_2 = 2.17, \mu_1^{max} = 1.34 [h^{-1}], \mu_2^{max} = 1.45 [h^{-1}] \\ k_n &= 1.57 [g.L^{-1}], k_s = 0.0154 [g.L^{-1}], k_e = 14.1 [g.L^{-1}] \end{aligned} \quad (41)$$

As shown on Fig. 3 in [13] the trajectories simulated with this parameter set fit well the experimental data of the batch fermentation.

For the control law and the Kalman Filter, we used the following parameter values: $\forall i = 1 : 4$,

$$a_{i,1} = 1.2 [h^{-1}], a_{i,2} = 0.25 [h^{-2}], \sigma = 0.2 \text{ and } \varepsilon = 0.64. \quad (42)$$

For the set of parameters (41), the constant inlet flow values Q_i^{OL} , $i = 1 : 4$, which lead at equilibrium to the setpoint (35) have been computed and are given by:

$$(Q_1^{OL}, Q_2^{OL}, Q_3^{OL}, Q_4^{OL}) = (0.2016, 0.1541, 0.0983, 0.0755). \quad (43)$$

These inlet flow values fulfill the constraint (36), which makes the setpoint (35) reachable.

The impact of the saturation order on the stabilization time has been evaluated through numerical simulations, in the noise-free case (see table III). The quickest stabilization time is obtained for

TABLE III
STABILIZATION TIME AT 2% AND 5% FOR THE DIFFERENT SATURATION ORDERS IN CLOSED LOOP AND FOR THE OPEN LOOP CONTROL LAW.

	Saturation order in closed loop				Open loop
	{10, 11, 12, 13, 14}	{4, 5}	{2, 7}	{1, 3, 6, 8, 9}	
2%	8.0	8.2	8.6	15.9	43.8
5%	6.6	6.7	6.9	14.0	30.6

the saturation orders $n^{\circ}10$ to 14. The Anti-windup Input-Output Linearization control law gives better results than the open-loop control law in terms of stabilization time. However the difference between closed loop and open loop varies depending on the chosen setpoint, the closed loop control law being always at least as fast as the open-loop control law⁵.

For the experiments, the order $n^{\circ}14$ has therefore been chosen.

⁵The minimal time synthesis for the control of the yeast biomass (and not the one of the sugar) in a MSCF with only two reactors has been studied in [17]. It presents bang-bang and singular arcs which makes it sensitive to error measurements and therefore difficult to implement in practice.

TABLE IV
SUGAR CONCENTRATIONS MEASUREMENT DATA.

Measurement time [h]	Sugar concentrations [g.L ⁻¹]			
	S ₁	S ₂	S ₃	S ₄
0	185.8	161.5	140.4	58.6
23.0	174.56	140.69	108.19	69.1
38.7	174.77	140.10	106.32	66.9

TABLE V
SUGAR CONCENTRATION SETPOINTS AND FINAL MEASUREMENTS,
VOLUMES AND INITIAL DILUTION RATES OF THE EXPERIMENT.

Reactor number	Sugar concentration [g.L ⁻¹] with S ₀ = S ₀ [*] = 202 g.L ⁻¹					
	S _i [*]	S _i	S _i - S _i [*]	δ _i [*] := S _i [*] - S _{i-1} [*]	δ _i := S _i - S _{i-1}	δ _i - δ _i [*]
1	170	174.77	4.77	32	27.23	-4.77
2	140	140.10	0.1	30	34.67	4.67
3	110	106.32	-3.68	30	33.78	3.78
4	70	66.9	-3.1	40	39.42	-0.58

Some simulations obtained with this saturation order are shown in Fig. 6. For these simulations, we considered noisy measurements of the CO₂ production rates, the measurement noise having a zero-mean normal distribution with standard deviation $\sigma = 0.1$.

In Fig. 6 (top), the sugar concentration obtained with the Anti-windup Input-Output linearization control law is compared to the one obtained with the constant input flow rates Q^{OL}. We see that the MSCF is stabilizing at the setpoint with both the closed loop and open loop control laws, but that the stabilization time is smaller with the closed-loop strategy as it was already shown in table III. In Fig. 6 (middle), the values of the control input are plotted: we can verify that the constraint (1) is fulfilled all along the simulation. Finally, the noisy measurement values of the CO₂ production rate are shown in Fig. 6 (bottom).

In these simulations, the parameter sets used for the simulation of the MSCF and for the control law are different and the measurements of the CO₂ production rate are noisy. It shows that the Anti-windup Input-Output Linearization control law is robust to both parameter uncertainties and measurement noise.

D. Experimental results

The same experiment as the one tested in simulation has been performed on the real process. The sugar concentration in each reactor has been measured before applying the control law: the measurement values (given in table IV, time 0) have been used for the initialization of the Kalman filter. During the experiment, two other off-line measurements of the sugar concentration have been made at 23.0 h and 38.7 h respectively (see table IV).

The experimental results are presented in Fig. 7. The estimated sugar concentrations given by the observer are first plotted in Fig. 7 (top). In Fig. 7 (middle and bottom) are given the computed control input values Q_i and the on-line measurement of the CO₂ production rates C_i.

The measurements of the final sugar concentrations are given in Table V for comparison with the setpoint values. As we can see, the qualitative behaviour of the control law is good and similar to the one obtained in numerical simulation. However, without any on-line sugar concentration measurement, it is not possible to completely cancel the control error, which is even though smaller than 4.77 g.L⁻¹ in all the reactors. The uncertainty on sugar measurements being 3%, the control error that is equal to 2.8%, 0.07%, 3.5% and 4.4% in the 4 reactors is reasonable.

E. Importance of the value of Sⁱⁿ for the control error

Because of the cascade structure of the system, the control strategy proposed in this paper does not really control the sugar concentration in each reactor, but rather the differences of sugar concentration between 2 consecutive reactors. The comparison between the values of the difference between consecutive setpoints and measurements are given in Table V. We can see that the control errors are different if we look at the sugar concentration values or at the difference of sugar concentration values between 2 consecutive reactors. For the second reactor for example, the control error on the sugar concentration is only 0.1 g.L⁻¹ whereas the control error on the difference of sugar concentration with the first reactor is equal to 4.67 g.L⁻¹.

In fact, as the sugar concentration is not directly controlled, it implies that the control error on the sugar concentration in the ith reactor will depend on the control error of the preceding reactor (the (i - 1)th reactor). To illustrate that, we can have a look at an other experiment performed on the MSCF that we have presented in the conference paper [13]. In this experiment (see Table 2 of [13]), the control error on the sugar concentration was larger than 6 g.L⁻¹ for all the reactors, whereas the control error on the difference of sugar concentration was smaller than 2.1 g.L⁻¹ for all the reactors except for the first one for which the error was equal to 6.1 g.L⁻¹. In that case, the control error on the sugar concentration of the first reactor was clearly impacting the errors made on the other reactors.

As we suspected, the large control error obtained for the first reactor in this experiment was the consequence of both the variation of the yield coefficient k₂ during the fermentation (see section IV) and the underestimation of the quantity of CO₂ that is dissolved in the medium (see section VI-B). Indeed for this experiment we only decreased the value of Sⁱⁿ of 3 g.L⁻¹ whereas in the experiments presented in section VI-D, 10 g.L⁻¹ was subtracted.

VII. CONCLUSION

In the present paper, the control of the sugar concentration in a Multi-Stage Continuous Fermenter (MSCF) has been studied. The cascade structure of the system induces a constraint on the control inputs that are the input flow rates of each reactor: the inlet flow rate of one reactor is indeed necessarily lower than that of the preceding reactor. To solve this problem, a linearizing control law coupled with an observer (Kalman Filter) and an anti-windup mechanism was applied to the real process. The obtained results are convincing. However, because of the lack of on-line measurement of the sugar concentration, we noticed the sensitivity of the results to the value of the initial sugar concentration. This value is not always well-known and moreover it has to be corrected in order to take into account that a part of the produced CO₂ is dissolved in the medium. In order to make the control law more robust to this uncertainty, an adaptive control law could be proposed that would adjust on line the value of the initial sugar concentration. An other interesting perspective would be to test and compare other control strategies that have been recently proposed in [18], [19]. Finally, the next objective for the control of the MSCF will be to control both the sugar concentration and the CO₂ production rate in each of the reactor.

REFERENCES

- [1] G. Bastin and D. Dochain, *On-line estimation and adaptive control of bioreactors*. Amsterdam: Elsevier, 1990.
- [2] G. Olsson and B. Newell, *Wastewater treatment systems: modelling, diagnosis and control*. IWA publishing, 1999.
- [3] P. Vigie, G. Goma, P. Renaud, G. Chamilotheoris, B. Dahhou, and J. Pourciel, "Adaptive predictive control of a multistage fermentation process," *Biotechnol. Bioeng.*, vol. 35, no. 3, pp. 217-223, 1990.

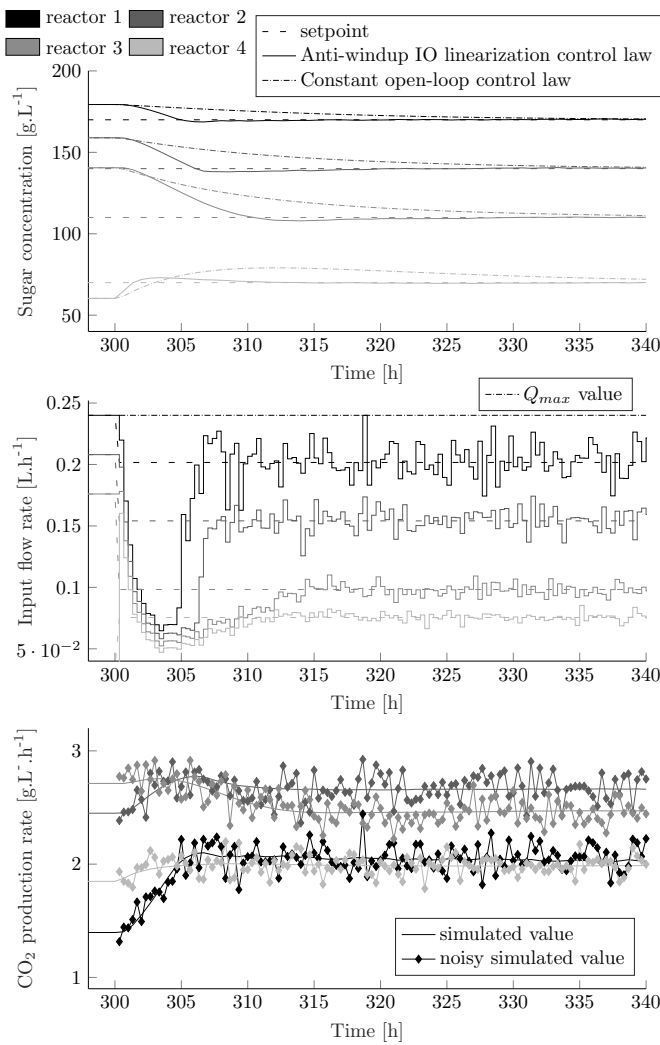


Fig. 6. Numerical results of the control of the sugar concentrations in the 4 reactors of the MSCF. Top: sugar concentration - comparison between open loop control and anti-windup Input-Output control. Middle: control input values. Bottom: CO₂ production rate values (real and noisy).

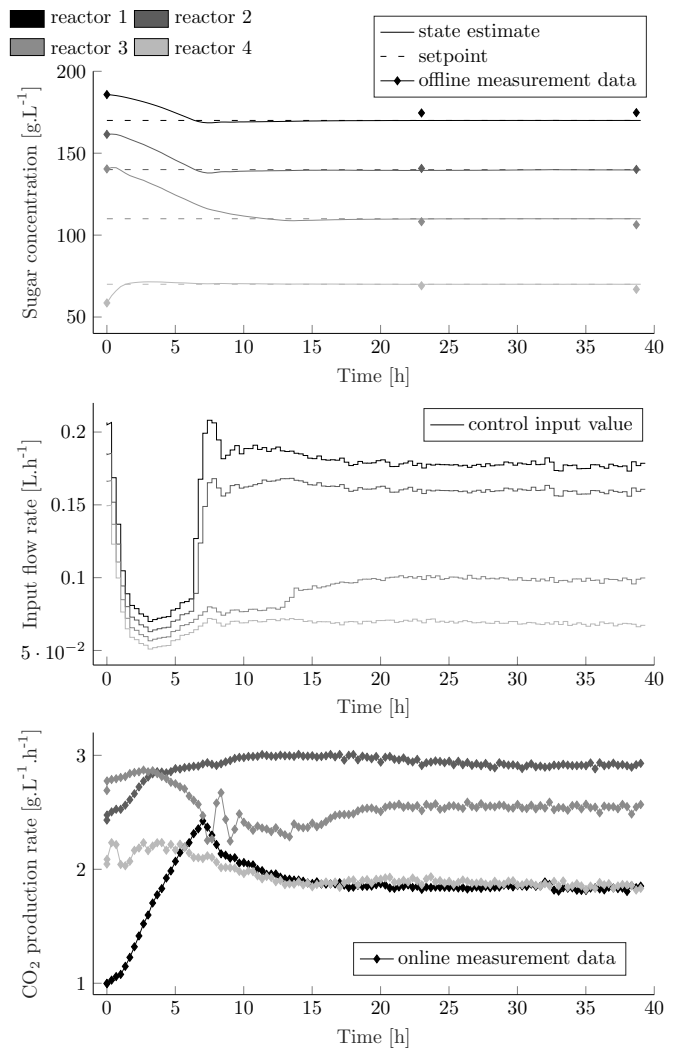


Fig. 7. Experimental results of the control of the sugar concentrations in the 4 reactors of the MSCF. Top: sugar concentration (setpoint, estimated value and offline measurements). Middle: control input values. Bottom: measurement values of the CO₂ production rate.

- [4] I. Simeonov, S. Stoyanov *et al.*, "Modelling and extremum seeking control of a cascade of two anaerobic bioreactors," *Int. J. Bioautomation*, vol. 15, no. 1, pp. 13–24, 2011.
- [5] C. de Gooijer, W. Bakker, H. Beefink, and J. Tramper, "Bioreactors in series: An overview of design procedures and practical applications," *Enzyme Microb. Tech.*, vol. 18, pp. 202–219, 1996.
- [6] S. Tarbouriech and M. Turner, "Anti-windup design: an overview of some recent advances and open problems," *IET Control Theory A*, vol. 3, no. 1, pp. 1–19, 2009.
- [7] F. Blanchini, "Set invariance in control," *Automatica*, vol. 35, pp. 1747–1767, 1999.
- [8] Y.-Y. Cao and Z. Lin, "Robust stability analysis and fuzzy-scheduling control for nonlinear systems subject to actuator saturation," *IEEE T Fuzzy Syst.*, vol. 11, no. 1, pp. 57–67, 2003.
- [9] S. Bezzaoucha, B. Marx, D. Maquin, and J. Ragot, "Stabilization of nonlinear systems subject to actuator saturation," in *Proc. FUZZ-IEEE 2013, Hyderabad, India*, 2013, pp. 1–6.
- [10] F. J. Doyle III, "An anti-windup input-output linearization scheme for SISO systems," *J. Process Contr.*, vol. 9, no. 3, pp. 213–220, 1999.
- [11] M. A. Henson and D. E. Seborg, *Nonlinear process control*. Upper Saddle River, New Jersey: Prentice-Hall PTR, 1997, ch. Feedback linearizing control, pp. 149–231.
- [12] A. Zheng, M. V. Kothare, and M. Morari, "Anti-windup design for internal model control," *Int. J. Control*, vol. 60, no. 5, pp. 1015–1024, 1994.
- [13] C. Casenave, D. Dochain, J. Harmand, M. Perez, A. Rapaport, and J.-M. Sablayrolles, "Control of a multi-stage continuous fermentor for the study of the wine fermentation," in *Proc. IFAC WC 2014, Cape Town, South Africa*, 2014, pp. 6192–6197.
- [14] T. Clement, M. Perez, J.-R. Mouret, J.-M. Sablayrolles, and C. Cama-rasa, "Use of a continuous multistage bioreactor to mimic winemaking fermentation," *Int. J. Food Microbiol.*, vol. 150, no. 1, pp. 42–49, 2011.
- [15] R. David, D. Dochain, J.-R. Mouret, A. Vande Wouwer, and J.-M. Sablayrolles, "Dynamical modeling of alcoholic fermentation and its link with nitrogen consumption," in *Proc. CAB 2010, Leuven, Belgium*, 2010, pp. 496–501.
- [16] J.-P. Corriou, *Process control: Theory and Applications*. Springer, 2004.
- [17] T. Bayen, A. Rapaport, and M. Sebbah, "Minimal time control of the two tanks gradostat model under a cascade input constraint," *SIAM J. Control Optim.*, vol. 52, no. 4, pp. 2568–2594, 2014.
- [18] C. Casenave and M. Perez, "Control of a class of nonlinear cascade systems with input-dependent saturations," in *Proc. CCDC 2015, Qingdao, China*, 2015, pp. 131–136.
- [19] C. Casenave and E. Montseny, "Simplification of dynamic problems by time-scale transformation: application to the nonlinear control with input positive constraints," in *Proc. IFAC WC 2017, Toulouse, France*, 2017, pp. 10 691–10 696.